

Current Status of Platinum Based Nanoparticles: Physicochemical Properties and Selected Applications – A Review

Platinum-based nanoparticles in electrochemistry, photochemistry and sensors

C. Sakthivel**, **L. Keerthana and I. Prabha***

Department of Chemistry, Bharathiar University, Coimbatore - 641 046, India

Email: *iprabha2007@gmail.com and **chemsakthifriend@gmail.com

The present article reviews the synthesis routes and applications of platinum-based nanoparticles in emerging fields such as energy harvesting, health care applications and sensors. Increasingly, more useful, novel and multifunctional materials are needed with fewer side effects. This article provides an overview of Pt-based nanoparticles along with recent applications in electrochemistry, photochemistry, biosensors and gas sensors. In particular, platinum dioxide (Adams' catalyst) has been used in many chemical reactions including hydrogenation, oxidation and reduction.

1. Introduction

An enormous number of metal oxide nanoparticles are utilised and appreciated for their unique properties and applications in the disciplines of nanoscience. Due to their distinct behaviour PtO₂ nanoparticles have significant catalytic activity. They were first prepared by Adams and are labelled Adams' catalyst (1). Adams' catalyst, or PtO₂, has been prepared mostly by colloidal techniques. The metal precursor produces an enhanced form of Pt catalyst after reduction with hydrogen. Finally there is the formation of stable Pt(0) in the form

of nanoparticles. This catalyst is used for further applications in chemical reactions.

PtO₂ has two different stable states: α-PtO₂ and β-PtO₂; α-PtO₂ has a hexagonal system at ambient pressure and β-PtO₂ has an orthorhombic system at high pressure (2). The β-PtO₂ displays more than one structure due to the presence of a larger amount of Pt³⁺ ions leading to the higher volume of β-PtO₂ and a smaller amount of oxygen. Pt⁴⁺ ions exhibit a tetragonal rutile structure in β-PtO₂ due to the maximum number of coulombic communications. Additionally, Pt³⁺ ions display an orthorhombic structure in β-PtO₂ due to the occurrence of high cationic interactions (3). Nanosized PtO₂ particles have revealed identical physical and chemical properties. Nano platina has been used to prepare novel materials for magnetic, high conductance, optical and thermal requirements for various specifications (4). Obviously, nanomaterials are currently of great interest, due to their potential physicochemical properties such as optoelectronic, electrical conductivity, mechanical strength, excellent magnetic and thermal properties. Materials having such properties might be introduced for various applications such as photocatalytic degradation, electrochemistry and biosensor applications and these factors are briefly described in this review.

1.1 Platinum Nanoparticles in Nanomaterials

Pt nanoparticles incorporated with tin(IV) oxide nanomaterials were investigated for their electrocatalytic properties through the

electrochemical oxygen reduction reaction (ORR) (Pt/SnO₂ vs. glassy carbon electrode). Electrochemical assessment showed that the Pt loaded electrode exhibited good activity for the ORR due to its high surface area (5). Pt supported on carbon having a large surface area is used as the cathode in polymer electrolyte fuel cells (PEFCs). However, Pt/SnO₂ nanowires have produced higher ORR activity than Pt/C, due to the low surface area of Pt/C as a reference catalyst in the ORR (6). Recently, galvanic exchange reactions have been used to synthesise different types of nanomaterials such as alloys, bimetallic nanoparticles and noble metals like Pt, gold and palladium with heterostructural morphology (7). Cobalt nanoparticles have acted as structure-inducing agents to achieve various kinds of morphology in metals and metal oxide nanomaterials including nanotubes, nanorods, nanowires and nanospheres (8).

Novel Pt-based nanoparticles having excellent physicochemical properties have been prepared with metals such as Pd, lead and iron. Pt nanoparticles were combined with Pd to form a 'dandelion like' surface morphology of core-shell nanoparticles. These Pt@Pd core-shell nanoparticles have been used as a highly active catalyst for olefin reduction reactions (9). The Pt@Pd core-shell nanoparticles have also been encapsulated with reduced graphene oxide (rGO) by microwave techniques. The resulting catalyst (Pt@Pd/rGO) had good physicochemical properties and has been used as a catalyst for dehalogenation in aromatic reactions through reduction of olefins with 98% improvement in yield and selectivity. The catalyst was further reusable more than five times in dehalogenation and reduction reactions of olefins. Noble metal-based nanoparticles such as Au@Cu, Au@Pd and Pd@Cu have comparatively good catalytic activity due to their size, surface area and morphology (10) and have been used as catalysts in organic reactions (11, 12). Pt nanoparticles incorporated into other materials have exhibited potential catalytic improvements (13) and can be easily synthesised through physical methods. There has been much focus on graphene oxide (GO) and rGO based core-shell nanomaterials including metal/GO and metal/rGO catalysts for methanol oxidation, metal salt reduction and electrocatalysis, due to their high activity, large surface area, superior electrical conductivity, high stability and recyclability (14). The modification of graphene into GO and rGO through oxidative exfoliation can lead to inadequate surface functionality due to its hydrophobic nature. Because GO and rGO are hydrophilic in nature, the

stability of core-shell nanomaterials is maintained. In Pt@Pd/rGO core-shell nanoparticles, a tendency for dehalogenation reactions has been observed with dehalogenation reaction following the order $F \ll Cl < Br < I$ (15).

1.2 Structural Properties

PtO₂ structures were established as tetragonal PtO, Pt₃O₄, Pt₅O₆, Pt₃O₈ and PtO₂ as determined by X-ray diffraction (XRD) spectroscopy (16). The structural elucidation of PtO₂ as β -PtO₂ (cadmium iodide type, space group Pnmm) (17) and α -PtO₂ was confirmed to be a hexagonal close packed structure (CdI₂ type, space group P-3m1) (18). XRD was used to determine the lattice parameter of α -PtO₂ film: $a = 3.113 \text{ \AA}$, $c = 4.342 \text{ \AA}$ and lattice parameter of α -PtO₂ powder: $a = 3.10 \text{ \AA}$ and $c = 4.29\text{--}4.41 \text{ \AA}$ (19). β' -PtO₂ has a rutile type structure (space group P42/mnm) (3). PtO₂ has an octahedral structure, formed from amalgamation of Pt in six-fold axis and oxygen in three-fold axis. The oxidation state of PtO₂ has been found to be +4 and PtO is considered to be +2 which implies a GeS-type structure, even though the Pt atom was six-fold. The Pt-Pt bond length in Pt₂ was found to be 2.33 \AA (20). Vacancy produces magnetism from oxide combined materials such as calcium oxide (21), zinc oxide (22), magnesium oxide (23), titanium dioxide (24), tin(IV) oxide (25) and hafnium(IV) oxide (26) to group III-nitrides (for example, gallium nitride and boron nitride) (27) and magnetic behaviour has also been established in diamond, graphite and graphene (28). Generally, oxides and nitrides of Pt occupy 2p orbitals or an open d shell with cation/anion vacancies, therefore PtO₂ (β -PtO₂) has vacancies which stimulate intrinsic magnetism due to the occurrence of the β phase.

The β -PtO₂ structure was found to be similar to the calcium chloride type crystal structure and to the TiO₂ type crystal structure with distortion (29). The Vienna *Ab initio* Simulation Package (VASP) was used to calculate the vacancy sites in the crystal system through plane wave and projector augmented wave method (PAW) potential. The plane wave energy was more than 600 electron volts (eV) (30). Coulomb repulsion (U_{eff}) plays an important role in band gap energy and β -PtO₂ has higher resistivity compared to α -PtO₂ with resistivity values of 10^6 \Omega cm and 10^4 \Omega cm respectively (31), however two different oxygen vacancies corresponding to PtO_{1.958} and PtO_{1.986} were $\delta = 0.042$ and $\delta = 0.014$ respectively. The energy

value between Fermi levels is an unoccupied state at approximately 31 meV and clearly depicts the transformation of electrons from one system into another vacancy state of a and b crystal system (32). There are numbers of planes of α -PtO₂ with area identified using the Joint Committee on Powder Diffraction Standards (JCPDS) card, with the planes (0001) and (1010) found to be more stable (33). When excited, the oxygen vacancy in α -PtO₂ (0001) and changes in surface area lead to distortion structure as shown in **Figure 1(a)**, **Figure 1(b)** and **Figure 1(c)**.

1.3 Chemical Reactivity

Heterogeneous catalysts have higher catalytic activity than homogeneous catalysts due to the presence of a large surface area. Additionally, sintered particles of PtO₂ possess different activation energies of 3.77 eV to Pt (bulk material) and -2.05 eV to Pt (gas), which depend upon the size of the nanoparticles. High sintering temperatures greater than 427°C provide more entropic driving force for vaporisation due to the low pressure of unstable particles (34). In recent research, the reaction of oxygen on metals such as cobalt, nickel, zinc, copper, Pt and Pd has been used to reduce atmospheric pollution. PtO₂ increases the chemical reactivity of CoO/CoAl₂O₄. The percentage of three capping materials has shown good reactivity in CoO/CoAl₂O₄, (CoO + 1.0% PtO₂)/CoAl₂O₄ and (CoO + 1.0% Rh₂O₃)/CoAl₂O₄, whereas time of reduction reaction was reduced by the addition of PtO₂ (35). PtO₂ has been applied to a wide range of chemical reactions such as hydrosilylation of olefins (alkenes) (36), defined as the addition of silicon and hydrogen on

an unsaturated double bond (C=C) or triple bond (C≡C) (37). PtO₂ as a heterogeneous catalyst for the hydrosilylation reaction can be easily removed compared to homogeneous catalysts. Homogeneous catalytic reactivity was first carried out by Karstedt using H₂PtCl₆ and Pt (PPh₃)₄ after which it was labelled as Karstedt's catalyst (38). The hydrosilylation reaction was studied using proton nuclear magnetic resonance (¹H-NMR) spectroscopy with the ratio of the Si-H singlet of silane at 4.7 ppm and the Si-CH₃ singlet of the product at 0.5 ppm (39).

1.4 Effects of Temperature and Air

There are many factors affecting the chemical reaction of metal oxides, such as atmospheric oxygen, the presence of impurities and time. Temperature is one of the most important factors and PtO₂ dissociates at a temperature of around 427°C (3). At 400°C, PtO₂ decomposes to Pt and O₂. A mixture of PtO₂ and carbon in helium decomposed at 550°C, as determined by differential thermal analysis (DTA), the same as PtO₂/He. When heated to 750°C Pt oxide lost weight as determined by thermogravimetric analysis (TGA), whereas Pt/C produced an exothermic reaction in the presence of He and air at high temperature enhanced by oxygen (40). Normally, transition metals easily corrode during oxidation reactions due to the presence of atmospheric oxygen in air. In a similar way Pt undergoes structural changes at the surface in the presence of air at pressure 0.025 bar to 1000 bar (41, 42). Hence, Pt metal can be treated in air or oxygen at high temperature of 400°C to 500°C to convert directly metal into gas using critical temperature which leaves the vicinity of the

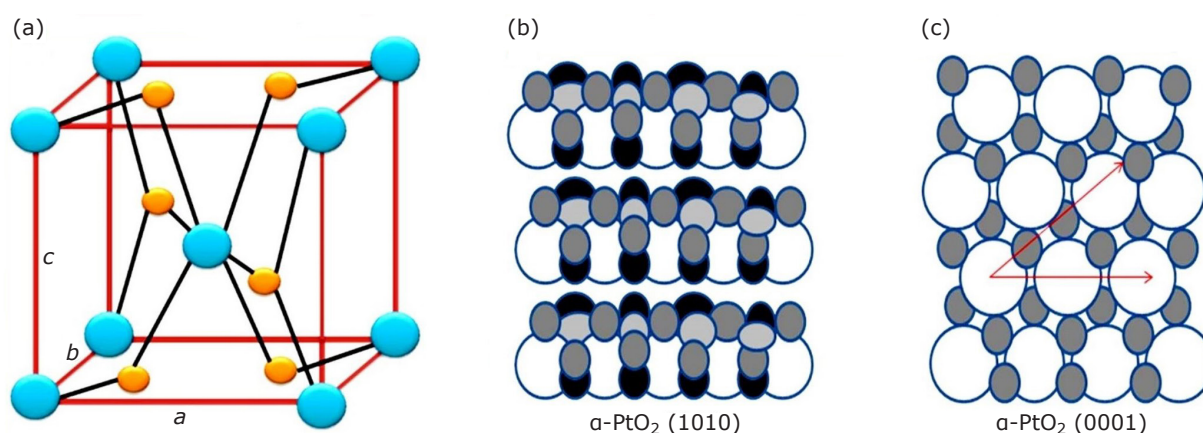


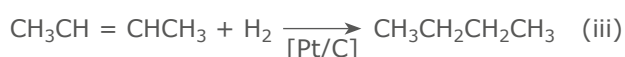
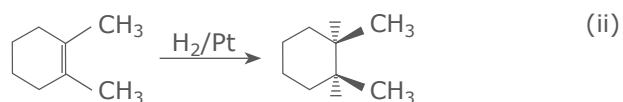
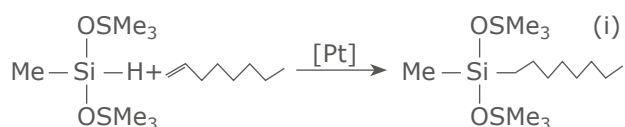
Fig. 1. (a) Crystal structure of PtO₂; (b) α -PtO₂ (1010); (c) α -PtO₂ (0001)

metal (43). In the presence of air with Na₂O-PtO₂ composition a monoclinic cell, space group C₂/c, with a = 5.411 Å, b = 9.386 Å and β = 99°39' and orthorhombic and monoclinic cell structure with general formula A₂BO₃ were determined by XRD spectroscopy (44).

2. Applications

2.1 Effective Catalyst in Organic Reactions

Pt is a transition metal with heterogeneous catalytic activity for specific chemical reactions such as removal of hydrogen, transfer of hydrogen and addition of oxygen, as shown in Equations (i)–(iii). In addition, Pt nanoparticles have high surface area and well defined catalytic performance (39). The transition metals Ni and Pd have similar characteristics to Pt nanoparticles. 0.05–2 wt% Pt nanoparticles were mixed with mesoporous silicas (SBA-15 and KIT-6) and aqueous ammonium tetrachloroplatinate(II) and calcined at 500°C to achieve Pt nanoparticles (45, 46). The same size nanoparticles were produced with different crystal systems due to the presence of catalyst to modify their structure (46). The catalytic activities of reaction sites for nanoparticles are dependent on both shape and crystalline facets in different orientations. Some facets exhibit higher catalytic activity than others, due to the involvement of oxygen on the Pt(100) plane and reduction on the Pt(111) plane (47, 48). Pt nanoparticles have been used as a catalyst in reaction with γ-Al₂O₃ to form nanoparticles of diameter around 0.2–0.8 nm before the elimination of polymer in O₂ at 375°C following the deposition and annealing process, as determined by scanning transmission electron microscopy (STEM) and extended X-ray absorption fine structure (EXAFS) (46). Supported Pt nanoparticles exhibit enhanced catalytic properties in the electro-oxidation of methanol due to increase in surface area of the Pt catalyst, which undergoes annealing to form smaller nanoparticles (49–51).



Supported Pt nanomaterials have been used in heterogeneous catalysts, with increased catalytic activity in the oxide phase (18). γ-Alumina doped with 1.5 wt% Pt is susceptible to poisoning by reactants such as nitric oxide, sulfur dioxide and hydrocarbons that could be eliminated at high temperature. The Pt nanoparticles were used as material dopant with Al₂O₃ for preparation of 2-propanol by an oxidation route, while the same kind of doped substance has produced conversion of more than 80% for the formation of acetone, carbon dioxide and water (46, 52, 53).

2.2 Photocatalysts

Generally, photocatalyst materials are considered to retain their own lifetime efficiently. Photocatalytic degradation of alcohols was studied using a PtO₂/TiO₂ nanocomposite (54–56). Transition metals ensure high electron capture between the conduction and valence band gap for photocatalytic performance (57). PtO₂ has been used to improve the photocatalytic activity of Ti-based materials. With increased Pt content of 1 wt% to 2 wt% the degradation was 61% and 51%, respectively. PtO₂ nanoparticles instead of Pt improved the degradation of phenol using sunlight efficiently (58). XRD study confirmed the percentage of phenol degradation for the given samples and the results showed that PtO and PtO₂ nanoparticles produced 67.5% and 32.5% of photodegradation respectively. The oxidation states of the metal play a vital role in photocatalytic degradation due to the presence of oxidation states such as Pt⁰, Pt²⁺, and Pt⁴⁺ (57) and the stability of the metal oxide depended on the number of oxygens present (18, 59). The order of photocatalytic activity and stability of PtO₂ are given below in (a) and (b) respectively.

(a) Photocatalytic reactivity order Pt⁰/PtO₂/TiO₂ > TiO₂ > PtO₂/TiO₂

(b) Stability of PtO₂ order Pt₃O₄ > Pt₂O₃ > PtO₂ > PtO

The photocatalytic performance of PtO₂ has been investigated with Pt⁰ formed during the CO oxidation reaction and positive potential of α-PtO₂. It has twenty times greater catalytic activity compared to Pt⁰/TiO₂ in the presence of sunlight (60). Two different forms of PtO₂, α-PtO₂ and β-PtO₂, were prepared by various techniques but the physicochemical properties of α-PtO₂ are still not well understood (2). α-PtO₂ nanoparticles suspended in ethanol have been maintained for 20 days without interruption and the sample

was examined by gas chromatography to find the chromatographic peaks. α -PtO₂ nanoparticles showed outstanding durability for months at ambient temperature without a stabiliser (61). Pt/PtO₂ metal nanoparticles have exhibited activity for catalytic application in several reactions including reduction of organic substrates such as substituted phenol, pyridine derivative, methyl ethyl ketone, vanillin and salicylaldehyde (62). Recent research has presented easy ways to identify the photocatalytic efficiency of PtO₂ compared with TiO₂ and PtO₂/TiO₂ based materials (57, 63–65).

2.3 Catalysts in Electrochemistry

Pt/PtO₂ catalysts can be applied in the field of electrochemistry. PtO₂ has a high electron density compared to Pt metal, which can act as a nucleophile and react with electrophiles. Pt/PtO₂ has very strong stability in acidic medium during electrolysis at high potential, as studied by mass spectrometry (66). Pt/PtO₂ nanoparticles with particle size of 8 nm showed high catalytic activity compared to bulk Pt/PtO₂ due to their high surface area (67) and showed enhanced catalytic activity for the hydrogen evolution reaction (HER) with improved particle size control (66). Pt nanoparticles have been used as electrocatalysts in a wide range of applications such as chemical and petrochemical industries, automobiles and fuel cells (68). Pt nanoparticles were used for the manufacture of supported nanopore materials particularly

in bipolar electrochemistry. It can be used for fluorescence in electrochemical microscopy. Bipolar electrochemistry is an important aspect of electrochemistry. A reaction is placed between two electrodes. One electrode works as an anode to oxidise the molecules and the other electrode acts as the cathode responsible for the reduction of molecules (69, 70). There are two types of bipolar cells in electrochemistry, open and closed bipolar cells (71). Such bipolar systems are prepared using nanomaterials such as nanoparticles, nanowires, nanorods and nanofilms (72). Pt nanoparticles were used to construct a nanoporous electrode by a focused ion-beam driven deposition technique and Pt nanoparticles were used in a coupled electrochemical cell prepared by focused ion-beam deposition. The supported Pt nanoparticles acted as the electrodes in electrochemical reaction with the help of a potentiostat which is shown in **Figure 2**.

Pt nanoparticles and nanoporous materials were reacted with gallium ions to fabricate nanoelectrodes with precise size and shape by a high focused beam technique and milling process. Conducting materials such as carbon, gold and tungsten were used to prepare electrodes for electrochemical reactions in which Pt acted as a highly efficient electrode due to its high stability, surface activity and electrocatalytic activity (73–75). Pt nanoparticles showed enhanced activity in the methanol oxidation reaction and have been used with supporting oxide materials in various fields such as catalytic supports (76),

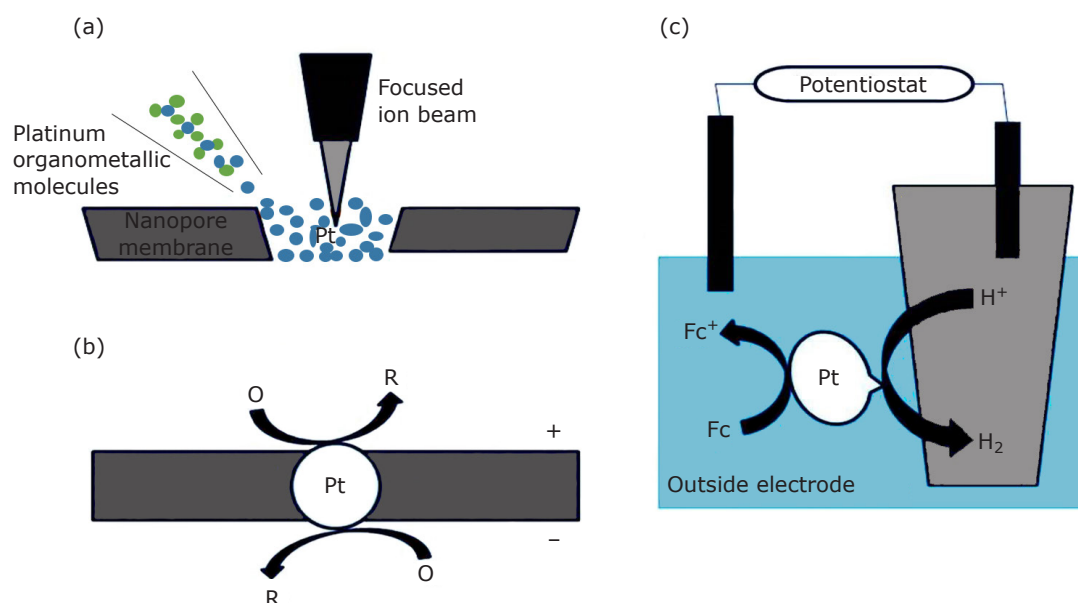
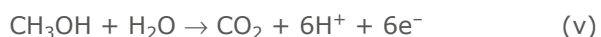


Fig. 2. (a) Construction of nanopore for focused ion-beam driven deposition technique; (b) coupled electrochemical focused ion-beam deposition; (c) supported Pt nanoparticles in electrochemical reaction

magnetic materials (77), photocatalysts (78, 79) and electronic systems (80).

Fe₂O₃ nanoparticles were found to perform well as catalysts due to their physicochemical properties. Fe₂O₃ supported by Pt (Fe₂O₃/Pt) materials have been used as an electrocatalyst for ORRs because of their high surface area, as shown in Equations (iv)–(vi) for the methanol electro-oxidation reaction (81, 82). **Figure 3** depicts the formation of Fe₂O₃ nanoparticles with supported Pt core-shell structure.



2.4 Biosensors

Pt nanoparticles are extensively used in biosensor applications, due to their wide range of magnetic properties (83, 84). Transition metals like Fe, Co and Ni, having magnetic characters, can be alloyed

with Pt to form stable metal alloys such as Pt-Fe, Pt-Co and Pt-Ni with different physical and chemical properties such as magnetic anisotropy for use in biosensor applications (85). Biosensor materials should maintain a pH range of 5.0–9.0 in dispersed solution and simultaneously the temperature should be kept at 95°C (86). Sensors can be used for applications such as measurement of blood sugar levels for diabetic patients, removal of pollutants in water, food production and biotechnology (87, 88). Immobilised glucose oxidase has been used to predict the concentration of glucose with the help of electrochemical biosensors due to its superior suitability and excellent sensitivity (89). In recent years fibre optic sensors have been fabricated with the help of Pt nanoparticles using localised surface plasmon resonance (LSPR). This principle has mainly focused on chemical sensors and biosensors and is shown in **Figure 4**. LSPR sensing properties are based on size and shape. Therefore, sensitivity was increased with decreasing particle size and sensitivity was decreased with increasing particle size (for example 10 nm to 50 nm).

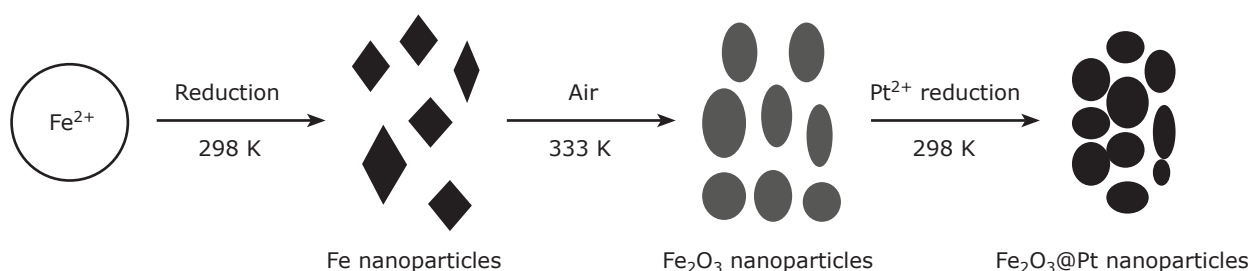


Fig. 3. Formation of Fe₂O₃ nanoparticles with supported Pt core-shell structure

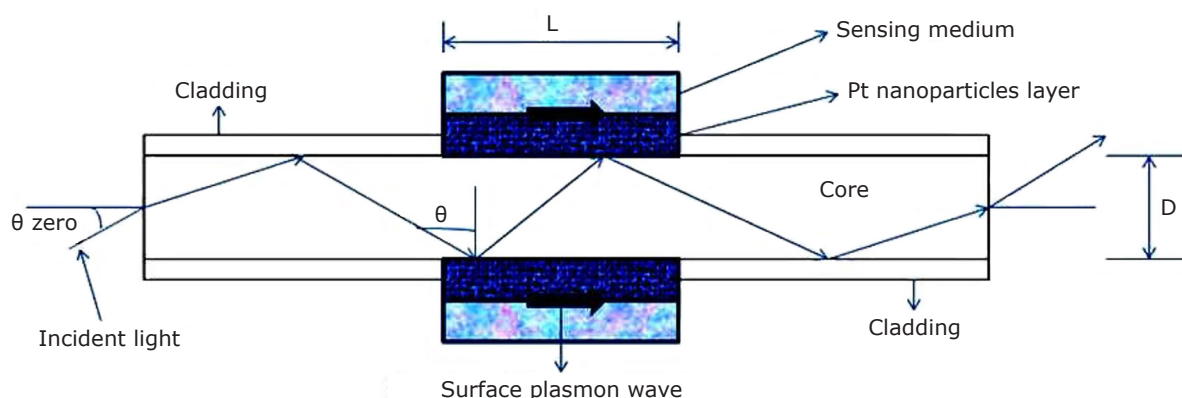


Fig. 4. Diagram for fibre optic sensor based on LSPR

Surface plasmon resonance (SPR) techniques have been used to investigate surface contact and sensing of liquids as well as other materials (90). Optical fibre was used for various purposes such as simplified and flexible optical design, remote sensing, continuous analysis or monitoring all based on SPR (91). Smaller size metal particles have comparatively high sensing and optical properties (92). Hence Pt metal is not only used in sensor applications but is also applicable in diverse fields such as optoelectronic devices, solar energy, jewellery (93), sensor materials, fuel cells, automotive applications, petroleum refining processes, hydrogen production and biomedical applications (94, 95).

Bisphenol A (BPA, 2,2-bis(4-hydroxyphenyl) propane), is used to manufacture polycarbonate and epoxy resin based plastics for food containers, water packets and plastic based medical containers. The nil effect concentration of BPA presented in drinking water and sea water values has been reported as $1.5 \mu\text{g l}^{-1}$ and $0.15 \mu\text{g l}^{-1}$ respectively (96, 97). BPA has been implicated in human health problems such as breast cancer, birth defects, infertility, diabetes and obesity (98, 99). Electrochemical sensors have been used to detect BPA through the oxidation reaction (100), by the presence of certain materials such as carbon (101), metal oxides and metals to activate electrodes (102–104). There is a need to find catalytic materials to increase the sensor activity

by direct oxidation with no electrode side effects using materials such as carbon and metals such as Pt (105–107).

A new electrode system has been prepared with a porous dual-Pt leaf inside the outward top scanning electrode and inward bottom scanning electrode. A simple arrow indicates the dissemination transportation in the direction of the actively scanning electrode in **Figure 5**. A membrane between the Pt leaves is used to prevent short circuits during the redox process, as shown in **Figure 6** (108). Various factors play an important role for the enhancement of sensing capability, although surface area was found to be the main feature to increase sensor activity. For example, soft Pt provides low sensitivity and reduced selectivity for an enzymatic glucose sensor (109).

2.5 Functionalised Materials in Gas Sensor

Generally, sensors can detect nearby objects. Sensors are classified based on the nature of materials. The first type are physical sensors based on energy sources such as thermal, magnetic and mechanical energy. The second type are chemical sensors which can detect chemicals present in the body, atmosphere or environment. Gas sensors are an essential part of present day life due to the presence of various harmful or easily explosive gases such as isopropanol (IPA), methane, ethanol,

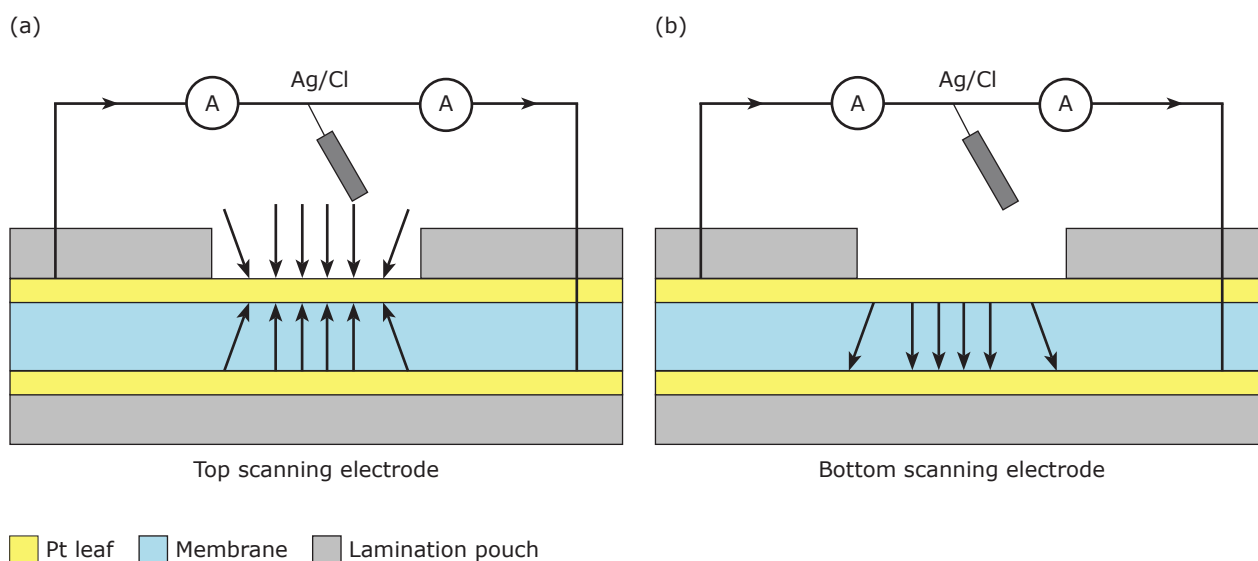


Fig. 5. (a) Dual-Pt leaves in outward top scanning electrode; (b) dual-Pt leaves in inward bottom scanning electrode. Reprinted from (108), with permission from Elsevier

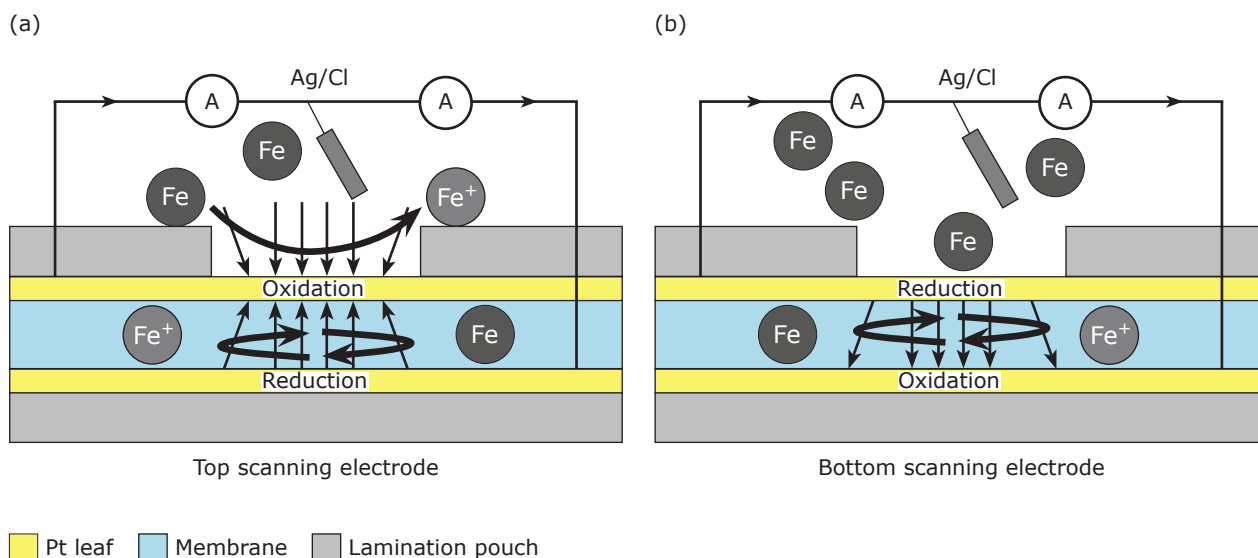


Fig. 6. (a) Diagram of top scanning electrode; (b) diagram of bottom scanning electrode. Reprinted from (108), with permission from Elsevier

methanol, formaldehyde, hydrogen, ammonia, hydrogen sulfide, nitrogen dioxide, sulfur dioxide and carbon monoxide, which cause health issues to human beings such as chronic bronchitis, emphysema and irritation, while high level concentrations can produce effects on the central nervous system, nausea and interior haemorrhage. Pt functionalised SnO₂ sheets have been used to detect IPA with a range of response values of 190.50 for 100 ppm of IPA at a controlled temperature of 220°C. It has excellent physicochemical properties and low cost, easy fabrication, high sensitivity and environmental safety (110).

In 2010 almost 665 gas leakages were recorded in Japan, including over 50 explosions. 60% of gas leakages were in residential areas. Therefore, gas sensors are essential to measure the gas and there are several materials already in use. These include platinum oxide (PtO_x) on graphene quantum dots on titania (GQDs/TiO₂) nanocomposite which behaves as a gas sensor to detect the highly aromatic volatile organic compound IPA with a sensor response range of more than 4.4 for a minimum concentration of 1 ppm and response within 9 seconds at room temperature. In addition, TiO₂ nanoparticles exhibit good surface area, unique optoelectronic properties, are easy to synthesise and have a narrow band gap. It can be coupled with graphene quantum dots as the composite materials acting as the gas sensors. Pt modified GQDs/SnO₂ thin film shows a transition from P-type to n-type sensing behaviour to sense

acetone gas at room temperature with excellent results (111). Therefore, conjugated materials with the addition of metals and metal oxides such as Pt, Pd, Ni, PtO₂ and SnO₂ respectively can be used to enhance the gas sensing ability. A simple schematic diagram for a gas sensor which contains an alumina tube, sensor and test circuit are shown in **Figure 7** (112, 113).

3. Conclusions and Future Work

Nanomaterials play an important role in the fields of materials science, the medical industry, engineering and the polymer industry. This review article has covered selected applications of photocatalysts, electrochemical catalysts, biosensors and gas sensors. Further research work on nanosized Pt/PtO₂ will study areas like the stability of Pt materials, environmental aspects, biocompatibility, non-toxicity, suitability for various applications, electrochemical activity and chemical reactivity. There is currently interest in Pt/PtO₂ materials for emerging energy applications as it can produce excellent power conversion in various electrochemical applications such as fuel cells, batteries, capacitors, supercapacitors and solar materials, which were not covered in detail here. In fuel cells Pt plays a crucial role in electrochemistry as a counter electrode, due to no or minimum loss of energy conversion. Nanoscale Pt/PtO₂ is being used for removal of pollutants like sulfur and methane from industry and residential

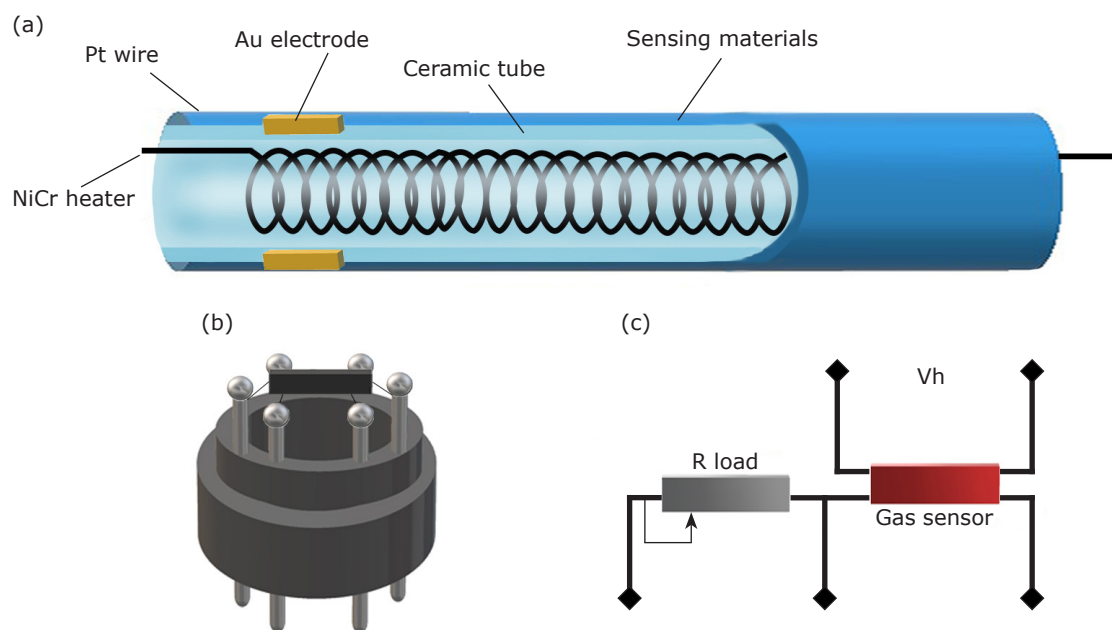


Fig. 7. Schematic diagrams of (a) alumina tube; (b) sensor; (c) test circuit. Reprinted from (112), with permission from Elsevier

areas and of CO₂ from the polymer industry and heavy-duty vehicles. In addition, it is used for the elimination of toxic and heavy metals such as lead, chromium and arsenic from the environment and from sewage or other waste waters, which can be purified by bio-sensing and electrochemical purification techniques for further usage including drinking if it meets water level recommendations and for agrochemical processes. Pt and PtO₂ based nanomaterials are also of great interest for future applications in spacecraft engines and low weight material applications due to their high ductility and thermal resistance properties. Pt and PtO₂ nanomaterials also behave as active catalysts in various chemical reactions, due to large surface area and porosity, particularly in the oxide form PtO₂ which is also under investigation for doping with other metals and alloys such as PtO₂-Pt, PtO₂-Fe and PtO₂-Co.

References

1. F. Bernardi, M. C. M. Alves and J. Morais, *J. Phys. Chem. C*, 2010, **114**, (49), 21434
2. O. Muller and R. Roy, *J. Less Common Metals*, 1968, **16**, (2), 129
3. L. K. Ono, B. Yuan, H. Heinrich and B. R. Cuenya, *J. Phys. Chem. C*, 2010, **114**, (50), 22119
4. B. He, Y. Ha, H. Liu, K. Wang and K. Y. Liew, *J. Colloid Interface Sci.*, 2007, **308**, (1), 105
5. A. Rabis, D. Kramer, E. Fabbri, M. Worsdale, R. Kötzt and T. J. Schmidt, *J. Phys. Chem. C*, 2014, **118**, (21), 11292
6. A. Rabis, P. Rodriguez and T. J. Schmidt, *ACS Catal.*, 2012, **2**, (5), 864
7. G. Hu, N. Yang, G. Xu and J. Xu, *J. Appl. Geophys.*, 2018, **150**, 118
8. H. Li, B. Lin, W. Yang, C. Zheng, Y. Hong, Y. Gao, T. Liu and S. Wu, *Int. J. Coal Geol.*, 2016, **154-155**, 82
9. K. J. Datta, K. K. R. Datta, M. B. Gawande, V. Ranc, K. Čépe, V. Malgras, Y. Yamauchi, R. S. Varma and R. Zboril, *Chem. Eur. J.*, 2016, **22**, (5), 1577
10. A. Goswami, A. K. Rathi, C. Aparicio, O. Tomanec, M. Petr, R. Pocklanova, M. B. Gawande, R. S. Varma and R. Zboril, *ACS Appl. Mater. Interfaces*, 2017, **9**, (3), 2815
11. C.-F. Hsia, M. Madasu and M. H. Huang, *Chem. Mater.*, 2016, **28**, (9), 3073
12. H. M. Song, D. H. Anjum, R. Sougrat, M. N. Hedhili and N. M. Khashab, *J. Mater. Chem.*, 2012, **22**, (48), 25003
13. J. W. Hong, S. W. Kang, B.-S. Choi, D. Kim, S. B. Lee and S. W. Han, *ACS Nano*, 2012, **6**, (3), 2410
14. V. Georgakilas, M. Otyepka, A. B. Bourlinos, V. Chandra, N. Kim, K. C. Kemp, P. Hobza, R. Zboril and K. S. Kim, *Chem. Rev.*, 2012, **112**, (11), 6156
15. V. Georgakilas, J. N. Tiwari, K. C. Kemp, J. A. Perman, A. B. Bourlinos, K. S. Kim and R. Zboril, *Chem. Rev.*, 2016, **116**, (9), 5464

16. Y. Abe, M. Kawamura and K. Sasaki, *Jpn. J. Appl. Phys., Part 1*, 1999, **38**, (4A), 2092
17. Y. Nagano, *J. Therm. Anal. Calorim.*, 2002, **69**, (3), 831
18. N. Seriani, W. Pompe and L. C. Ciacchi, *J. Phys. Chem. B*, 2006, **110**, (30), 14860
19. J. Zhensheng, X. Chanjuan, Z. Qingmei, Y. Feng, Z. Jiazheng and X. Jinzhen, *J. Mol. Catal. A: Chem.*, 2003, **191**, (1), 61
20. N. Tian, Z.-Y. Zhou, S.-G. Sun, Y. Ding and Z. L. Wang, *Science*, 2007, **316**, (5825), 732
21. J. Osorio-Guillén, S. Lany, S. V. Barabash and A. Zunger, *Phys. Rev. Lett.*, 2006, **96**, (10), 107203
22. J. A. Chan, S. Lany and A. Zunger, *Phys. Rev. Lett.*, 2009, **103**, (1), 016404
23. J. Hu, Z. Zhang, M. Zhao, H. Qin and M. Jiang, *Appl. Phys. Lett.*, 2008, **93**, (19), 192503
24. M. V. Ganduglia-Pirovano, A. Hofmann and J. Sauer, *Surf. Sci. Rep.*, 2007, **62**, (6), 219
25. N. H. Hong, N. Poirot and J. Sakai, *Phys. Rev. B*, 2008, **77**, (3), 033205
26. C. Das Pemmaraju and S. Sanvito, *Phys. Rev. Lett.*, 2005, **94**, (21), 217205
27. P. Dev, Y. Xue and P. Zhang, *Phys. Rev. Lett.*, 2008, **100**, (11), 117204
28. J. J. Palacios, J. Fernández-Rossier and L. Brey, *Phys. Rev. B*, 2008, **77**, (19), 195428
29. K.-J. Range, F. Rau, U. Klement and A. M. Heyns, *Mater. Res. Bull.*, 1987, **22**, (11), 1541
30. G. Kresse and J. Furthmüller, *Phys. Rev. B*, 1996, **54**, (16), 11169
31. M. C. Jung, H.-D. Kim, M. Han, W. Jo and D. C. Kim, *Jpn. J. Appl. Phys., Part 1*, **38**, (8), 4872
32. Y. Yang, O. Sugino and T. Ohno, *Phys. Rev. B*, 2012, **85**, (3), 035204
33. T. M. Pedersen, W. X. Li and B. Hammer, *Phys. Chem. Chem. Phys.*, 2006, **8**, (13), 1566
34. E. M. Larsson, J. Millet, S. Gustafsson, M. Skoglundh, V. P. Zhdanov and C. Langhammer, *ACS Catal.*, 2012, **2**, (2), 238
35. H. Hong, H. Zhang, T. Han, F. He and H. Jin, *Energy Procedia*, 2017, **114**, 344
36. C. W. Scheeren, J. B. Domingos, G. Machado and J. Dupont, *J. Phys. Chem. C*, 2008, **112**, (42), 16463
37. 'Hydrosilylation of Alkynes and Their Derivatives – Regio- and Stereoselective Hydrosilylation of Alkynes Catalysed by Late Transition Metal Complexes', in "Hydrosilylation – A Comprehensive Review on Recent Advances", Vol. 1, ed. B. Marciniec, Springer Science and Business Media BV, Dordrecht, The Netherlands, 2009, p. 57
38. N. Sabourault, G. Mignani, A. Wagner and C. Mioskowski, *Org. Lett.*, 2002, **4**, (13), 2117
39. S. Putzien, E. Louis, O. Nuyken and F. E. Kühn, *Catal. Sci. Technol.*, 2012, **2**, (4), 725
40. K. Kinoshita, *Thermochim. Acta*, 1977, **20**, (3), 297
41. J. Singh, M. Nachtegaal, E. M. C. Alayon, J. Stötzler and J. A. van Bokhoven, *ChemCatChem*, 2010, **2**, (6), 653
42. B. L. M. Hendriksen, S. C. Bobaru and J. W. M. Frenken, *Catal. Today*, 2005, **105**, (2), 234
43. Y.-S. Hu, Y.-G. Guo, W. Sigle, S. Hore, P. Balaya and J. Maier, *Nature Mater.*, 2006, **5**, (9), 713
44. C. L. McDaniel, *J. Solid State Chem.*, 1974, **9**, (2), 139
45. A. F. Lee, J. N. Naughton, Z. Liu and K. Wilson, *ACS Catal.*, 2012, **2**, (11), 2235
46. S. Mostafa, F. Behafarid, J. R. Croy, L. K. Ono, L. Li, J. C. Yang, A. I. Frenkel and B. R. Cuenya, *J. Am. Chem. Soc.*, 2010, **132**, (44), 15714
47. R. Xu, D. Wang, J. Zhang and Y. Li, *Chem. – An Asian J.*, 2006, **1**, (6), 888
48. V. Komanicky, H. Iddir, K.-C. Chang, A. Menzel, G. Karapetrov, D. Hennessy, P. Zapol and H. You, *J. Am. Chem. Soc.*, 2009, **131**, (16), 5732
49. G. Gökağaç and B. J. Kennedy, *Zeitschrift für Naturforsch. B*, 2002, **57**, (2), 193
50. A. S. Aricò, A. K. Shukla, K. M. El-Khatib, P. Cretì and V. Antonucci, *J. Appl. Electrochem.*, 1999, **29**, (6), 673
51. D.-J. Guo and H.-L. Li, *J. Electroanal. Chem.*, 2004, **573**, (1), 197
52. J. H. Zhang, X. L. Zhou and J. A. Wang, *J. Mol. Catal. A: Chem.*, 2006, **247**, (1–2), 222
53. N. Burgos, M. Paulis, M. Mirari Antxustegi and M. Montes, *Appl. Catal. B: Environ.*, 2002, **38**, (4), 251
54. S. K. Parayil, H. S. Kibombo, C.-M. Wu, R. Peng, T. Kindle, S. Mishra, S. P. Ahrenkiel, J. Baltrusaitis, N. M. Dimitrijevic, T. Rajh and R. T. Koodali, *J. Phys. Chem. C*, 2013, **117**, (33), 16850
55. W. Y. Teoh, L. Mädler and R. Amal, *J. Catal.*, 2007, **251**, (2), 271
56. H. Wang, Z. Wu, Y. Liu and Y. Wang, *Chemosphere*, 2009, **74**, (6), 773
57. H. S. Kibombo, C.-M. Wu, R. Peng, J. Baltrusaitis and R. T. Koodali, *Appl. Catal. B: Environ.*, 2013, **136–137**, 248
58. F. B. Li and X. Z. Li, *Chemosphere*, 2002, **48**, (10), 1103
59. N. Seriani, Z. Jin, W. Pompe and L. C. Ciacchi, *Phys. Rev. B*, 2007, **76**, (15), 155421
60. A. V. Vorontsov, E. N. Savinov and J. Zhensheng, *J. Photochem. Photobiol. A: Chem.*, 1999, **125**, (1–3), 113
61. M.-R. Gao, Z.-Y. Lin, J. Jiang, C.-H. Cui, Y.-R. Zheng and S.-H. Yu, *Chem. – A Eur. J.*, 2012, **18**, (27), 8423

62. D. A. Svintsitskiy, L. S. Kibis, A. I. Stadnichenko, S. V. Koscheev, V. I. Zaikovskii and A. I. Boronin, *ChemPhysChem*, 2015, **16**, (15), 3318
63. B. Sun, A. V. Vorontsov and P. G. Smirniotis, *Langmuir*, 2003, **19**, (8), 3151
64. C. A. Emilio, M. I. Litter, M. Kunst, M. Bouchard and C. Colbeau-Justin, *Langmuir*, 2006, **22**, (8), 3606
65. B. Sun, P. G. Smirniotis and P. Boolchand, *Langmuir*, 2005, **21**, (24), 11397
66. M. Sarno and E. Ponticorvo, *Int. J. Hydrogen Energy*, 2017, **42**, (37), 23631
67. D. Miller, H. Sanchez Casalongue, H. Bluhm, H. Ogasawara, A. Nilsson and S. Kaya, *J. Am. Chem. Soc.*, 2014, **136**, (17), 6340
68. G.-Y. Zhao and H.-L. Li, *Appl. Surf. Sci.*, 2008, **254**, (10), 3232
69. J. P. Guerrette, S. M. Oja and B. Zhang, *Anal. Chem.*, 2012, **84**, (3), 1609
70. J. T. Cox, J. P. Guerrette and B. Zhang, *Anal. Chem.*, 2012, **84**, (20), 8797
71. S. E. Fosdick, K. N. Knust, K. Scida and R. M. Crooks, *Angew. Chem. Int. Ed.*, 2013, **52**, (40), 10438
72. A. Lundgren, S. Munktel, M. Lacey, M. Berglin and F. Björefors, *ChemElectroChem*, 2016, **3**, (3), 378
73. R. Hao and B. Zhang, *Anal. Chem.*, 2016, **88**, (1), 614
74. J. Clausmeyer and W. Schuhmann, *TrAC Trends Anal. Chem.*, 2016, **79**, 46
75. Y. Li, D. Bergman and B. Zhang, *Anal. Chem.*, 2009, **81**, (13), 5496
76. I. X. Green, W. Tang, M. Neurock and J. T. Yates, *Science*, 2011, **333**, (6043), 736
77. V. Subramanian, E. E. Wolf and P. V. Kamat, *J. Phys. Chem. B*, 2003, **107**, (30), 7479
78. S. Sato, R. Asahi, T. Morikawa, T. Ohwaki, K. Aoki and Y. Taga, *Science*, 2002, **295**, (5555), 626
79. R. K. Nagarale, U. Hoss and A. Heller, *J. Am. Chem. Soc.*, 2012, **134**, (51), 20783
80. J. W. Hennek, Y. Xia, K. Everaerts, M. C. Hersam, A. Facchetti and T. J. Marks, *ACS Appl. Mater. Interfaces*, 2012, **4**, (3), 1614
81. V. M. Dhavale and S. Kurungot, *J. Phys. Chem. C*, 2012, **116**, (13), 7318
82. S. M. Devi, A. Nivetha and I. Prabha, *J. Supercond. Novel Magn.*, 2018, *Review Paper*
83. J. B. Tracy, D. N. Weiss, D. P. Dinega and M. G. Bawendi, *Phys. Rev. B*, 2005, **72**, (6), 064404
84. S. Behrens, H. Bönnemann, N. Matoussevitch, A. Gorschinski, E. Dinjus, W. Habicht, J. Bolle, S. Zinoveva, N. Palina, J. Hormes, H. Modrow, S. Bahr and V. Kempter, *J. Phys.: Condens. Matter*, 2006, **18**, (38), S2543
85. X. Luo, A. Morrin, A. J. Killard and M. R. Smyth, *Electroanalysis*, 2006, **18**, (4), 319
86. I. L. Medintz, H. T. Uyeda, E. R. Goldman and H. Mattoussi, *Nature Mater.*, 2005, **4**, (6), 435
87. A. Heller and B. Feldman, *Chem. Rev.*, 2008, **108**, (7), 2482
88. L. Meng, J. Jin, G. Yang, T. Lu, H. Zhang and C. Cai, *Anal. Chem.*, 2009, **81**, (17), 7271
89. W.-Z. Jia, K. Wang, Z.-J. Zhu, H.-T. Song and X.-H. Xia, *Langmuir*, 2007, **23**, (23), 11896
90. J. Homola, *Sensors Actuators B: Chem.*, 1997, **41**, (1-3), 207
91. A. K. Sharma and B. D. Gupta, *Sensors Actuators B: Chem.*, 2004, **100**, (3), 423
92. S. Lal, S. Link and N. J. Halas, *Nature Photonics*, 2007, **1**, (11), 641
93. J. Hurly and P. T. Wedepohl, *J. Mater. Sci.*, 1993, **28**, (20), 5648
94. L. M. Velichkina, A. N. Pestryakov, A. V. Vosmerikov, I. V. Tuzovskaya, N. E. Bogdanchikova, M. Avalos, M. Farias and H. Tiznado, *Pet. Chem.*, 2008, **48**, (3), 201
95. A. Chen and P. Holt-Hindle, *Chem. Rev.*, 2010, **110**, (6), 3767
96. H. Yin, L. Cui, S. Ai, H. Fan and L. Zhu, *Electrochim. Acta*, 2010, **55**, (3), 603
97. G. M. Klečka, C. A. Staples, K. E. Clark, N. van der Hoeven, D. E. Thomas and S. G. Hentges, *Environ. Sci. Technol.*, 2009, **43**, (16), 6145
98. L. N. Vandenberg, R. Hauser, M. Marcus, N. Olea and W. V. Welshons, *Reprod. Toxicol.*, 2007, **24**, (2), 139
99. H. Mielke and U. Gundert-Remy, *Toxicol. Lett.*, 2009, **190**, (1), 32
100. K. V. Ragavan, N. K. Rastogi and M. S. Thakur, *TrAC Trends Anal. Chem.*, 2013, **52**, 248
101. J. A. Rather and K. De Wael, *Sensors Actuators B: Chem.*, 2013, **176**, 110
102. L. Hu, C.-C. Fong, X. Zhang, L. L. Chan, P. K. S. Lam, P. K. Chu, K.-Y. Wong and M. Yang, *Environ. Sci. Technol.*, 2016, **50**, (8), 4430
103. Z. Zheng, Y. Du, Z. Wang, Q. Feng and C. Wang, *Analyst*, 2013, **138**, (2), 693
104. R. Wannapob, P. Thavarungkul, S. Dawan, A. Numnuam, W. Limbut and P. Kanatharana, *Electroanalysis*, 2017, **29**, (2), 472
105. V. Malgras, H. Ataee-Esfahani, H. Wang, B. Jiang, C. Li, K. C.-W. Wu, J. H. Kim and Y. Yamauchi, *Adv. Mater.*, 2015, **28**, (6), 993
106. Q. Shen, L. Jiang, H. Zhang, Q. Min, W. Hou and J.-J. Zhu, *J. Phys. Chem. C*, 2008, **112**, (42), 16385
107. D.-S. Park, M.-S. Won, R. N. Goyal and Y.-B. Shim, *Sensors Actuators B: Chem.*, 2012, **174**, 45

108. H. R. Zafarani, L. Rassaei, E. J. R. Sudhölter, B. D. B. Aaronson and F. Marken, *Sensors Actuators B: Chem.*, 2018, **255**, 2904
109. I. T. Bae, E. Yeager, X. Xing and C. C. Liu, *J. Electroanal. Chem. Interfacial Electrochem.*, 1991, **309**, (1–2), 131
110. C. Dong, X. Liu, X. Xiao, G. Chen, Y. Wang and I. Djerdj, *J. Mater. Chem. A*, 2014, **2**, (47), 20089
111. S. Shao, Y. Chen, S. Huang, F. Jiang, Y. Wang and R. Koehn, *RSC Adv.*, 2017, **7**, (63), 39859
112. B. Yang, J. Liu, H. Qin, Q. Liu, X. Jing, H. Zhang, R. Li, G. Huang and J. Wang, *Ceram. Int.*, 2018, **44**, (9), 10426
113. N. Murata, T. Suzuki, M. Kobayashi, F. Togoh and K. Asakura, *Phys. Chem. Chem. Phys.*, 2013, **15**, (41), 17938

The Authors



C. Sakthivel is a PhD Research Scholar, under the guidance of I. Prabha at the Department of Chemistry, Bharathiar University, Coimbatore, India. His current laboratory research focuses on novel nanomaterials with catalysis, energy and biological based applications. He has received a BSc in Chemistry from Periyar University, Tamil Nadu, India and an MSc in Chemistry, Bharathidasan University, Tamil Nadu, India. Additionally, he has completed a Bachelors Degree in Education from Tamil Nadu Teacher Education University, Chennai, India. He has published a review paper in *Materials Today Sustainability*, published by Elsevier. He has presented a full-length paper in international conference proceedings and was awarded best paper presentation. He has work experience and knowledge in paints with applications in the PG project. He has attended various national and international conferences at various institutions.



L. Keerthana is an MPhil Research Scholar under the guidance of I. Prabha at the Department of Chemistry, Bharathiar University, Coimbatore, India. Her current laboratory research focuses on novel nanomaterials with catalysis, energy and biological based applications. She holds both undergraduate and postgraduate degrees in Chemistry. She has published a paper in *Materials Today Sustainability*. She has presented in national and international conferences. Her research area of interest is materials chemistry.



I. Prabha completed her MSc in Chemistry from Gandhigram Rural Institute, Dindigu, India and MPhil in Chemistry from Madurai Kamaraj University, Madurai, Tamil Nadu, India. She completed her PhD at the Department of Chemistry, Sathyabama University, Chennai, Tamil Nadu, India. She has worked as an Associate Professor at the Department of Chemistry, Bharathiar University, Coimbatore, India since November 2016. Her research focuses on the chemistry of nanomaterials and its recent applications, novel catalysts and advanced photocatalysis, green catalysis and its synthesis for societal benefits, water purification and quality assessment. She has published research articles in various national and international journals. She has presented and attended various international and national conferences, seminars and workshops. Currently she is guiding PhD and MPhil students. She has written book chapters for BE, BTech and MSc (Chemistry) students.